Supporting Information

Probing the biogenesis of polysaccharide granules in algal cells at sub-organellar resolution via Raman microscopy with stable isotope labeling

Yusuke Yonamine[a*], Takuya Asai[b], Yuta Suzuki[b], Takuro Ito[c,d,e], Yasuyuki Ozeki[b*], and Yu Hoshino[f*]

[a]*Research Institute for Electronic Science, Hokkaido University, Kita21, Nishi10, Kita-ku, Sapporo 001-0021, Japan*
[b]*Department of Electrical Engineering and Information Systems, The University of Tokyo, 7-3-1 Hongo, Bunkyo-ku, Tokyo 113-8656, Japan*
[c]*Department of Chemistry, The University of Tokyo, 7-3-1 Hongo, Bunkyo-ku, Tokyo 113-0033, Japan*
[d]*Japan Science and Technology Agency, 4-1-8, Honcho, Kawaguchi, Saitama 332-0012, Japan*
[e]*Department of Creative Engineering, National Institute of Technology, Tsuruoka College, 104 Sawada, Inooka, Tsuruoka, Yamagata 997-8511, Japan*
[f]*Department of Chemical Engineering, Kyushu University, 744 Motooka, Fukuoka 819-0395, Japan*

*E-mail: yonamine@es.hokudai.ac.jp, ozeki@ee.t.u-tokyo.ac.jp, yhoshino@chem-eng.kyushu-u.ac.jp

Table of Contents

Supporting Figures

Supporting figures

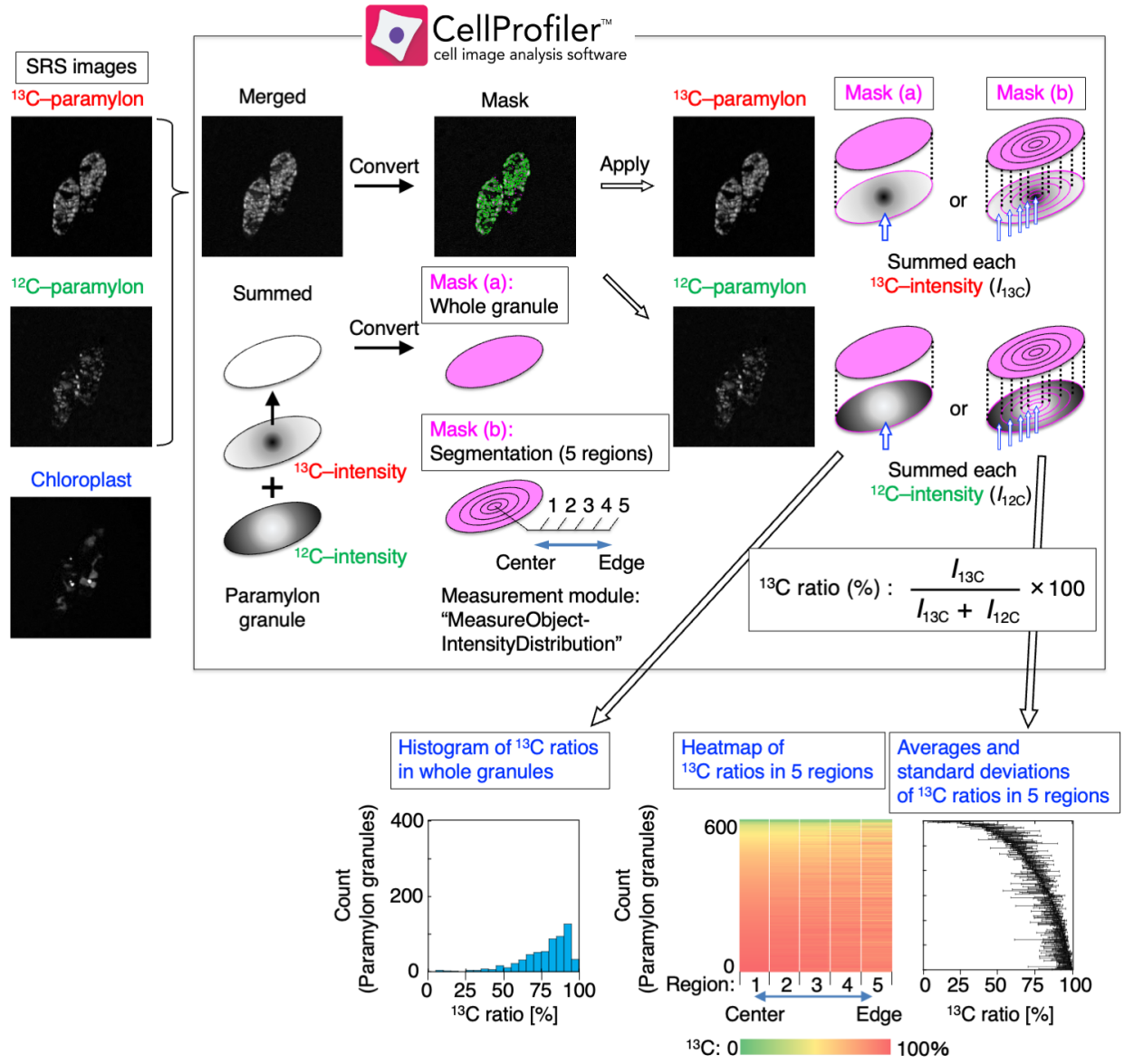

Figure S1. Procedure for analyzing the SRS images of the different ^{13}C ratios in the paramylon granules by the CellProfiler software.

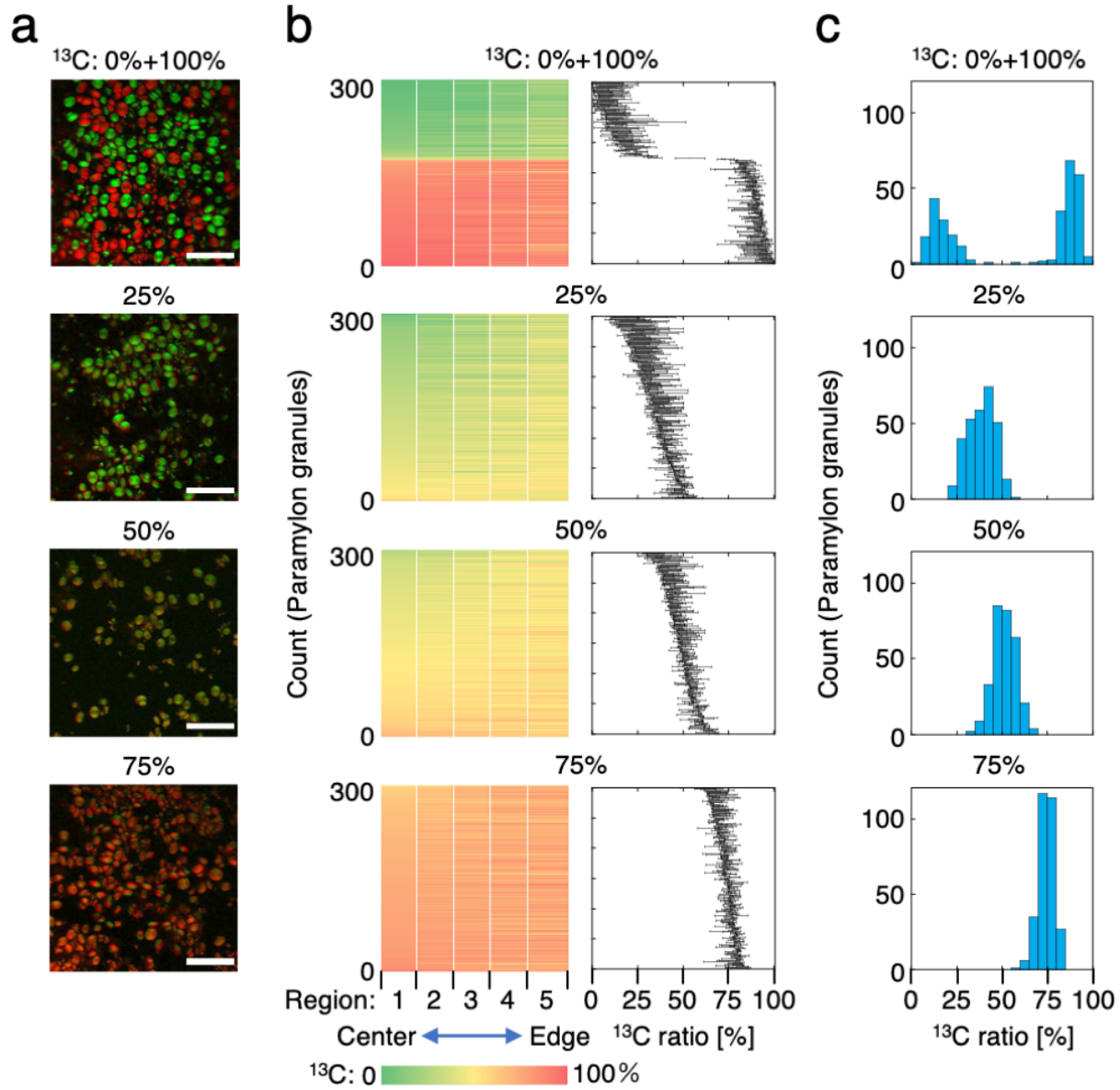

Figure S2. Statistical analyses of the SRS images for the ^{13}C ratios of the paramylon granules that were incubated by a mixture of the ^{13}C and ^{12}C sources. (a) Representative SRS images of the paramylon granules from Figure 3c. Scale bars: 10 μm. (b) Heatmaps (left) and average values with standard deviations (right) of the ^{13}C ratios in the five segmented regions (from the center to the periphery) of the individual paramylon granules (n = 300, randomly selected granules). (c) Histograms of the ^{13}C ratios in the whole paramylon granules. The ^{13}C ratios were calculated by analyzing the SRS images (n = 5, including the images in (a)).

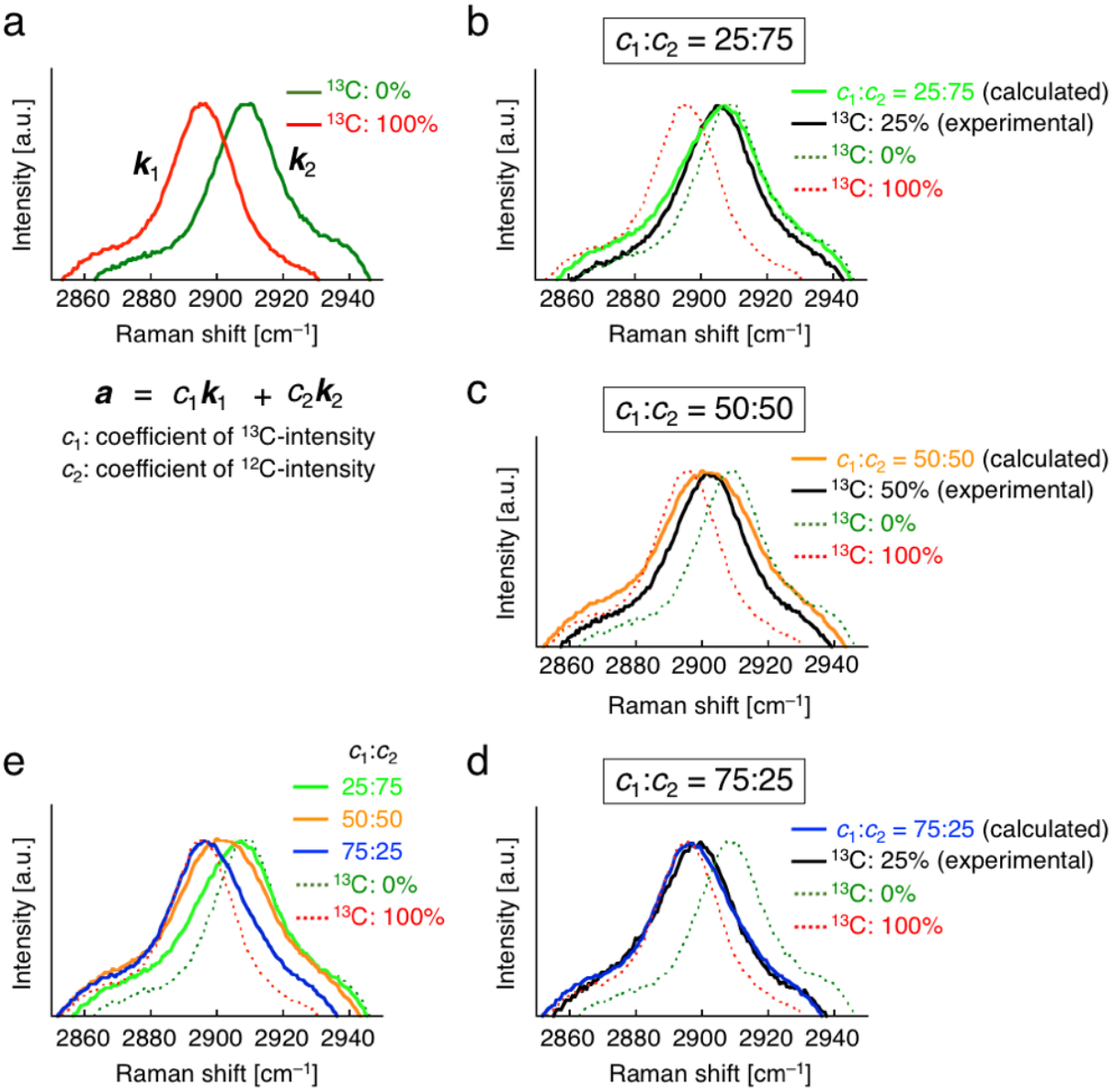

Figure S3. Comparison of the experimental Raman spectra in the CH stretching region of paramylon granules (incubated with the intermediate molar ratios of the ^{13}C and ^{12}C sources (^{13}C: 25, 50, and 75 mol%)) with the superposed spectra of the ^{13}C and ^{12}C paramylon granules at intensity ratios that correspond to the incubation ratios. (a) Enlarged views of the experimental spectra of the 100% ^{13}C– and 100% ^{12}C–paramylon granules (red and green, respectively) and their linear combinations at different ratios (c_1:c_2) corresponding to the incubation molar ratios (^{13}C:^{12}C = 25:75, 50:50, and 75:25). (b–d) Comparison of the experimental and superposed spectra. (b) c_1:c_2 = 25:75. (c) c_1:c_2 = 50:50. (d) c_1:c_2 = 75:25. The spectra are normalized at the maximum intensities. The 100% ^{13}C– and 100% ^{12}C–paramylon granules are also shown as the reference. (e) Overlaid spectra of the superposed spectra of b–d.

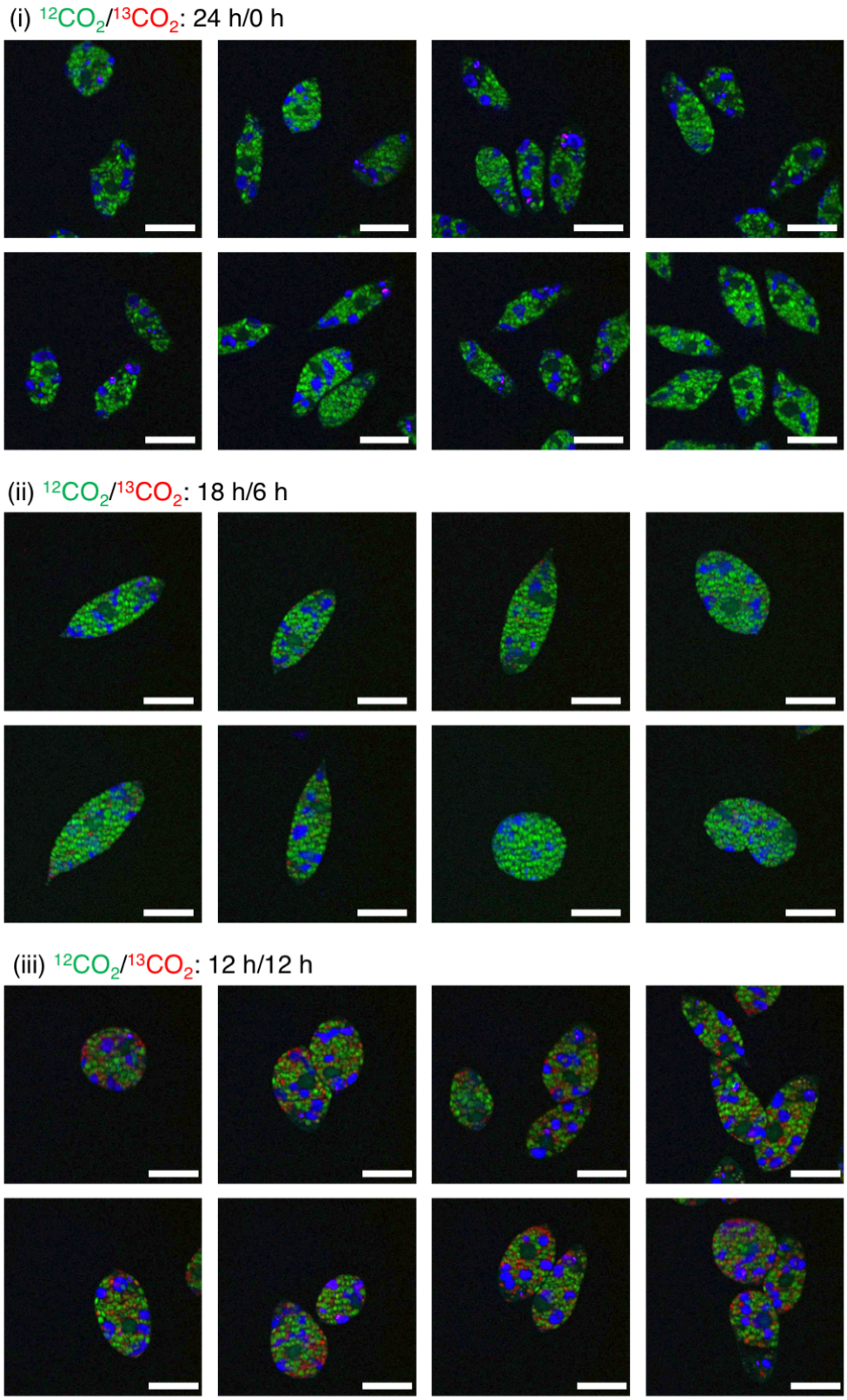

Figure S4. SRS images of the *E. gracilis* cells that were incubated under the conditions depicted in Figure 5a. Scale bars: 20 μm.

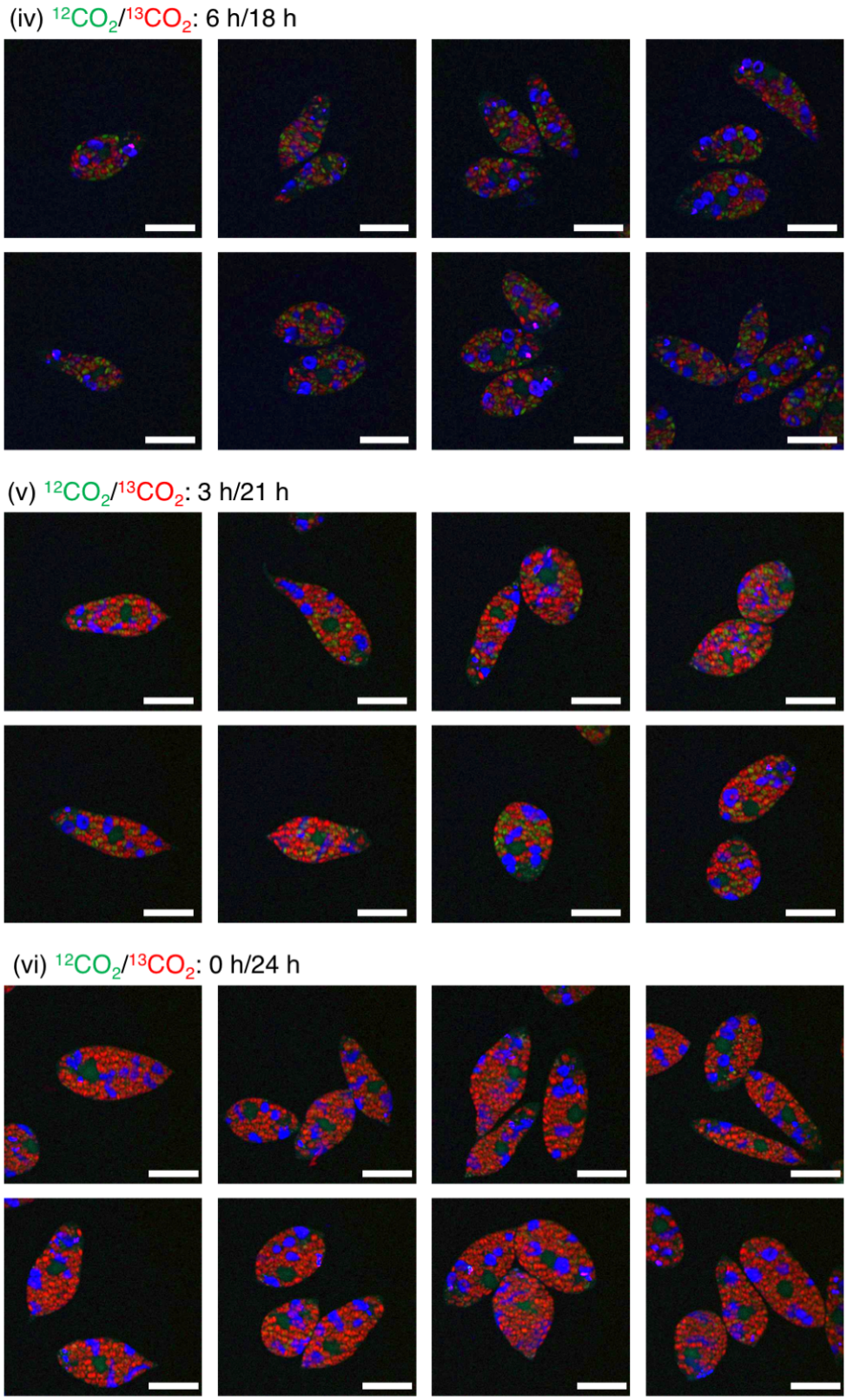

Figure S4 (continued). SRS images of the *E. gracilis* cells that were incubated under the conditions depicted in Figure 5a. Scale bars: 20 μm.

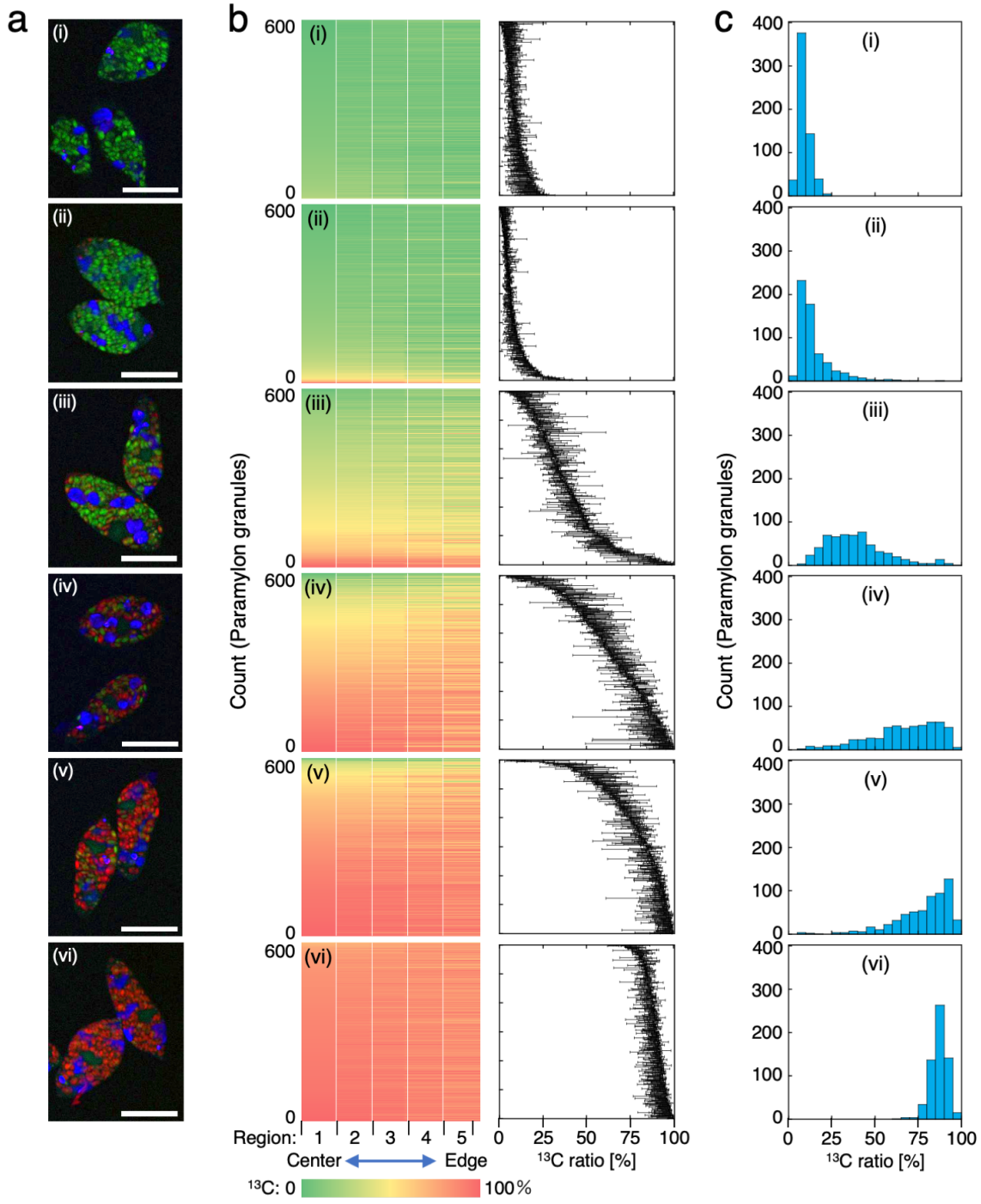

Figure S5. Statistical analyses of the SRS images for the ^{13}C ratios of the paramylon granules in the *E. gracilis* cells that were incubated under the conditions depicted in Figure 5a. (a) Representative SRS images of the *E. gracilis* cells from Figure 5b. Scale bars: 20 µm. (b) Heatmaps (left) and average values with standard deviations (right) of the ^{13}C ratios in the five segmented regions (from the center to the periphery) of the individual paramylon granules (n = 600, randomly selected granules). (c) Histograms of the ^{13}C ratios in the whole paramylon granules. The ^{13}C ratios were calculated by analyzing the SRS images (n = 9, including the images in (a) and Figure S4).

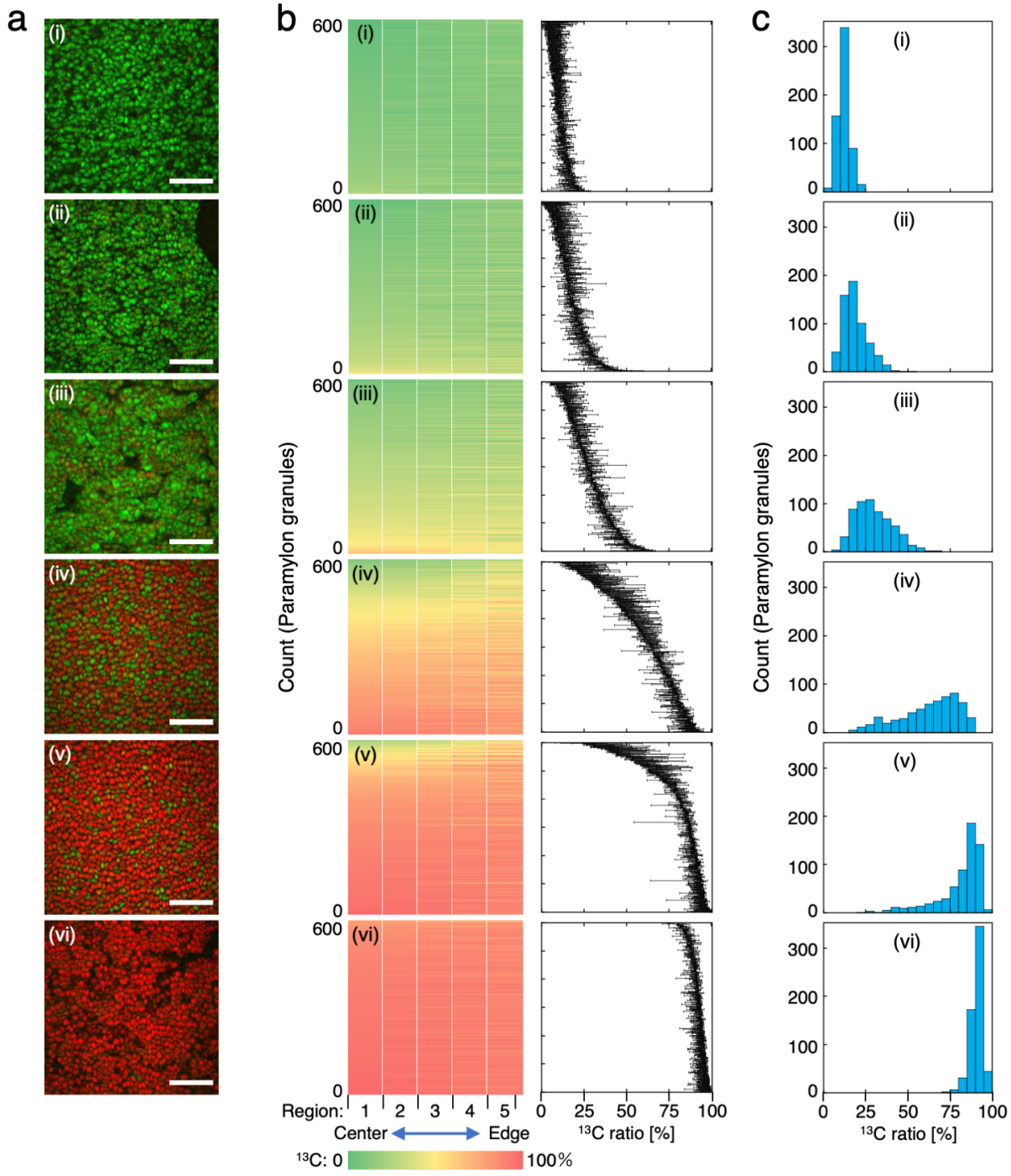

Figure S6. SRS imaging of the extracted paramylon granules that were incubated with atmospheric switching from the ^{12}C to ^{13}C source depicted in Figure 5a. (a) SRS images of the extracted paramylon granules that were incubated under the conditions depicted in Figure 5a. The ^{13}C and ^{12}C constituents were color-coded as red and green employing the spectra of the 100% ^{13}C– and 100% ^{12}C–paramylon granules in the RGB color model, respectively. Scale bars: 20 µm. (b) Heatmaps (left) and average values with standard deviations (right) of the ^{13}C ratios in the five segmented regions (from the center to the periphery) of the individual paramylon granules (n = 600, randomly selected granules). (c) Histograms of the ^{13}C ratios in the whole paramylon granules. The ^{13}C ratios were calculated by analyzing the SRS images in (a).

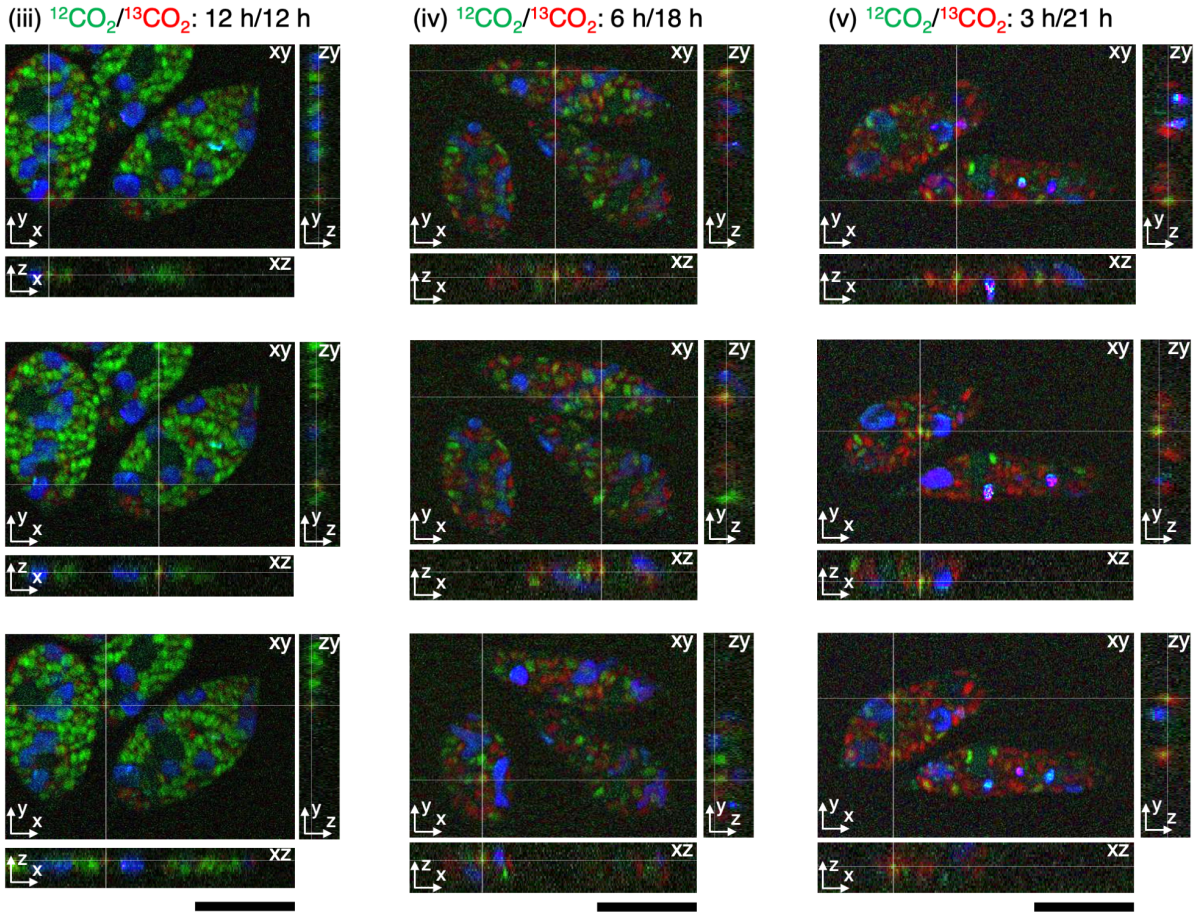

Figure S7. Cross-sectional analysis of 3D SRS imaging of the *E. gracilis* cells that were incubated under the conditions depicted in Figure 5a (iii)–(v). Scale bars: 20 µm. Scale bars: 20 µm. The ^{13}C and ^{12}C constituents, as well as the chloroplast in all the SRS images, correspond to the red, green, and blue color codes in the RGB color model, respectively, employing the spectra in Figure S9a.

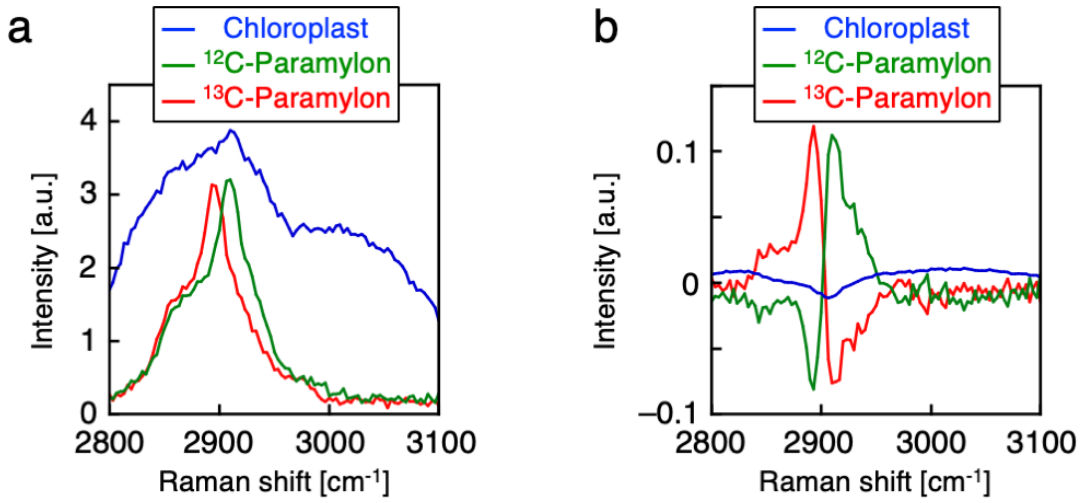

Figures S8. (a) Raman spectral bases of the three organelles (^{13}C– and ^{12}C–paramylon granules as well as the chloroplast) for analyzing the 2D SRS images of *E. gracilis* cells. The spectra were measured at 91 spectral points between 2800 and 3100 cm^{-1} (at intervals of 3.3 cm^{-1}). (b) Plots of the pseudo-inverse matrices corresponding to the Raman spectral bases in (a).

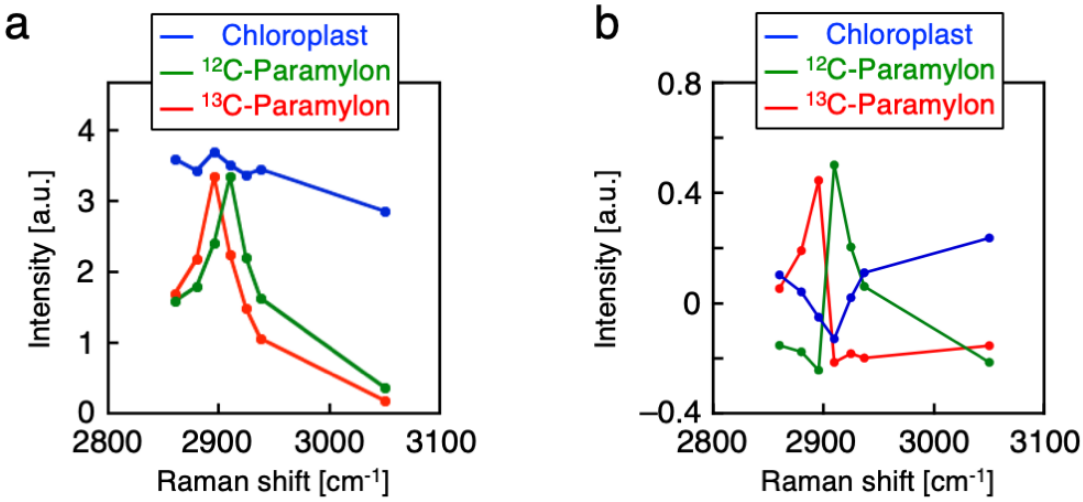

Figures S9. (a) Raman spectral bases of the three organelles (^{13}C– and ^{12}C–paramylon granules as well as the chloroplast) for analyzing the SRS images of *E. gracilis* cells in a three-dimensional structure. The spectra were measured at seven spectral points (2860, 2880, 2896, 2910, 2925, 2937, and 3050 cm^{-1}). (b) Plots of the pseudo-inverse matrices corresponding to the Raman spectral bases in (a).